NUMERICAL STUDY OF THE INITIAL PRESSURE AND DIAMETERS RATIO EFFECT ON THE JET EJECTOR PERFORMANCE

Sadoun Fahad Dahkil, Tahseen Ali Gabbar and Dhamia Khalf Jaber
Technical college of Basrah / Fuel and Energy Department

ABSTRACT

In this paper, computation fluid dynamics model (CFD) is used to simulate a turbulence flow fields along the jet ejector. A Steady-state 2-D compressible flow model utilities the standard *k-ε* turbulent model has been used. The performance of jet ejector is simulated by FLUENT 6.3 (code) and GAMBIT software, using finite-volume scheme to solve transport NAVIER STOKE equations. The objective of this study is to investigate the high-performance of jet ejector geometry (mass flow and head ratio) nozzle to throat diameter at eight cases (D_N/D_T) with different initial pressure. Research is performed to optimize jet performance by varying initial pressure and nozzle diameter ratios from (1/8) to (8/8).

To increase understanding of the axial velocity distribution at an important regions along the ejector, three regions are chosen, at inlet (1,3), nozzle exit(2) and midpoint of throat(4), with an important different diameters ratio cases 1,2,3,5,7 and 8 respectivly. The comparison of these results is presented by the axial velocity magnitude, mass and head ratio of the ejector at the above cases.

Results show that higher pressure ratio and mass ratio (high performance) occur when the nozzle to throat diameter ratio (D_N/D_T) was (5/8) and (1/8) respectively. Also mass ratio is decreased at all initial pressure when the diameter ratio increased.

Key word: fluid dynamic, internal flow, turbulence flow, CFD

دراسة عددية لتأثير الضغط الابتدائي ونسبة الاقطار على اداء لافظه هواء

الخلاصة:

تظمت الدراسة تحليل نظري للجريان المضطرب على طول مجرى لافظة هواء باستخدام نمذجة ديناميكا الموائع الحاسوبي. اعتبر الجريان بحالة مستقره وبعدين ولا انضغاطي مع استخدام نموذج الاضطراب (turbulent model *k-ε*) . تم نمذجة أداء لافظة الهواء باستخدام البرنامج العددي الجاهز(Gambit & Fluent) لحل المعادلات لتفاضلية الجزئية باستخدام نظرية الحجوم المحددة لحل المعادلات التفاضلية الجزئية.

تهدف الدراسة لتعين أفضل اداء (نسبة معدل الجريان ونسبة الضغط) للافظة الهواء بتغير نسبة الاقطار والضغط الابتدائي ولثمان حالات اختيرت لهذا الغرض. لغرض زيادة التحليل تم اختيار ثلاث مستويات على طول اللافظة وهي: بداية الدخول(1) وعند المنفث (nozzle exit)(2) وكذلك منتصف مجرى الخنق (D_T) (4) ولنسبة اقطار (1,2,3,5,7,8) يلاوتلا ىلع. للحصول على توزيع السرعة على طول المستويات المذكورة والمقارنه بقيم السرعه و نسبة الكتلة الداخلة (معدل السحب) والضغط .

بينت النتائج ان افضل نسبة انضغاط و الكتلة الداخلة (اداء عالي) عند نسبة اقطار 1/8, 5/8 على التوالي.

كذلك تبين النتائج ان نسبة الكتلة الداخلة تقل عند جميع قيم الضغط الابتدائي مع زيادة نسبة الاقطار.

Symbols

Symbol	Definition	SI Units
English symbols		
DN	nozzle diameter	M
DT	throat diameter	M
E	kinetic energy	J
K	turbulent kinetic energy	m^2/s^2
M	mass	kg
M	mass ratio	-
P	pressure	pa
RH	head ratio	-
T	temperature	K
T	time	s
V	velocity	m/s
Greek symbols		
Φ	dependent variable	-
ρ	density	kg/m3
ΓΦ	effective exchange variable coefficient of Φ	
Є	dissipation rate of turbulent energy	m^2/s^2
Subscribe		
1	nozzle inlet	
2	nozzle exit	
3	suction	
4	throat	
5	diffuser	

1-Introduction

Steam ejectors are designed to convert thee pressure energy of a motivating fluid too velocity energy at entrain suction fluid and then to recompress the mixed fluids by converting velocity energy back into pressure energy. This is based on the theory that a properly designed nozzle followed by a properly designed throat or venturi will economically make use of high pressure fluid to compress from a low pressure region to a higher pressure. This change from pressure head to velocity head is the basis of the jet vacuum principle.

Ejectors are generally categorized into one of four basic types: single-stage, multi-stage non-condensing, multi-stage condensing and multi-stage with both condensing and noncondensing stages.

Single-stage ejectors (shown in figure 1) are the simplest and most commonly used design. They are generally recommended for pressure from atmospheric to 3 inch Hg. Abs. Single-stage units typically discharge at or near atmospheric pressure. Multi-stage non-condensing ejectors are used where lower suction pressures are specified.

Jet ejectors provide numerous advantages, which are summarized below:

1. Jet ejectors do not require extensive maintenance, because there are no moving parts to break or wear.
2. Jet ejectors have lower capital cost comparing to the other devices, due to their simple design.
3. Jet ejectors are easily installed, so they may be placed in inaccessible places without any constant deliberation.

On the other hand, the major disadvantages of jet ejector are:

1. Jet ejectors are designed to perform at a particular optimum point. Deviation from this optimum point can dramatically reduce ejector efficiency.
2. Jet ejectors have very low thermal efficiency.

The applications of jet –ejector were important idea for many researchers as, Shengqiang Shen et al [1]

who studied a gas–liquid ejector and its application to a solar-powered bi-ejector refrigeration system. A new configuration of a bi-ejector refrigeration system is presented. The system incorporates two ejectors. The purpose of one is to suck refrigerant vapour from the evaporator and discharge to the condenser; the other acts as a jet pump to pump liquid refrigerant from the condenser to the generator. An analysis model for the bi-ejector refrigeration system and a one-dimensional flow model for the gas–liquid ejector were established. The performances of the gas–liquid ejector and the refrigeration cycle were studied using numerical modeling. The results show that the performances of ejector and system depends to a great deal on the refrigerants as well as on operation conditions.

Huang et al [2] studied theoretically and experimentally the 1-D ejector performance. A constant-pressure mixing is assumed to occur inside the constant-area section of the ejector and the entrained flow at choking condition is analyzed. They performed experiment using 11 ejectors and R141b as the working fluid to verify the analytical results. Their results show that the 1-D analysis using the empirical coefficients can accurately predict the performance of the ejectors. Mark J. BERGANDER [3] was developed a novel vapor compression cycle for refrigeration with regenerative use of the potential energy of two-phase flow expansion. The new cycle includes a second step compression by an ejector device, which combines the compression with simultaneous throttling of the liquid. The compressor compresses the vapor to approximately 2/3 of the final pressure and additional compression is provided in an ejector, thus the amount of mechanical energy required by a compressor is reduced and the efficiency is increased. The thermodynamic model was developed for R22 refrigerant, showing a possible efficiency improvement of 38% as compared to the traditional vapor compression cycle. Zhang and . Wang [4] designed a new continuous combined solid adsorption–ejector refrigeration and heating hybrid system driven by solar energy. The thermodynamic theory of the system was constructed, and the performance simulation and analysis were made under normal working conditions. Furthermore, under the same working conditions, they made a comparison with an adsorption system without an ejector with a COP of 0.3.Thier results showed that e the combined system's COP was improved by 10% totally and reached 0.33. Kanjanapon Chunnanond and Satha Aphornratana [5] provides a literature review on ejectors and their applications in refrigeration. A number of studies were grouped and discussed in several topics, i.e. background and theory of ejector and jet refrigeration cycle, performance characteristics, working fluid and improvement of jet refrigerator. Moreover, other applications of an ejector in other types of refrigeration system were also described. Hisham El-Dessouky et al [6] developed semi-empirical models for design and rating of steam jet ejectors. The model gave the entrainment ratio as a function of the expansion ratio and the pressures of the entrained vapor, motive steam and compressed vapor. Also, correlations were developed for the motive steam pressure at the nozzle exit as a function of the evaporator and condenser pressures and the area ratios as a function of the entrainment ratio and the stream pressures.

In this research the optimum jet-ejector geometry for each nozzle diameter ratio and motive pressure are investigated, CFD software (Fluent) is used to simulate flow fields in the jet ejector. Steady-state 2-D compressible flow using the standard k-ε turbulent model is utilized to solve the problem. Figure (1) show the graphical form of jet – ejector that will be studied in this research and the specifications of this jet – ejector are shown in table 1.

2-Basic Construction

Ejectors are composed of three basic parts: a nozzle, a mixing chamber and a diffuser as shown in Fig.(1). A high pressure motivating fluid enters at (1), expands through the converging-diverging nozzle to (2). The suction fluid (Mb) enters at (3), mixes with the motivating fluid in the mixing chamber (4). Both Ma and Mb are then recompressed through the diffuser to (5). The direct

entrainment of a low velocity suction fluid by a motive fluid results in an unavoidable loss of kinetic energy owing to impact and turbulence originally possessed by the motive fluid. Many factors affect jet ejector performance, including the fluid molecular weight, feed temperature, mixing tube length, nozzle position, throat dimension, motive velocity, Reynolds number, pressure ratio, and specific heat ratio[6].

Previous research attempted to study the effect of nozzle position on jet ejector performance. They found that the nozzle position had a great effect on the jet ejector performance, as it determines the distance over which the motive and propelled stream are completely mixed. ESDU (1986) suggested that the nozzle should be placed between 0.5 and 1.0 length of throat diameter before the entrance of the throat section. Holton (1951) studied the effect of fluid molecular weight, whereas Holton and Schultz (1951) studied the effect of fluid temperature.

A few literature researches have studied the effect of nozzle diameter on jet ejector performance. This is a major focus of our work. The optimum length and diameter of the throat section, the nozzle position, and the radius of the inlet curvature before a convergence section in a constant-area jet ejector design are investigated for each individual nozzle diameter. The nozzle diameter ratio, defined by *DN/D*T, is varied from (1/8) to (8/8). The pressure of motive fluid at nozzle exit is varied from (1 bar) to (5.5 bar).

The back pressure of the ejector is maintained constant at 101.3 kPa. Air is used as a working fluid. Once the geometry of the jet ejector is created, a grid can be mapped to it. This step is completed by grid-generating software (GAMBIT). To account for turbulent behavior, the standard *k-ε* model is selected. The ideal gas law is applied to calculate flow variables in the turbulent model. The wall boundary conditions are assumed to be adiabatic with no heat flux .

In this research, the optimum jet-ejector geometry for each nozzle diameter ratio and motive pressure were investigated using Fluent computational fluid dynamic (CFD) software. Fluent uses a mass-average segregated solver to solve the fundamental transport equations such as continuity, and momentum conservation for compressible, Newtonian fluid (Navier-Stokes equation). The governing equations are discretized in space using a finite volume differencing formulation, based upon an unstructured grid system.

3-Theoretical analysis:

In this paper, CFD software (FLUENT) is used to simulate flow field through the jet ejector. Steady state 2D compressible flow and using the standard *k-ϵ* turbulent model to solve the turbulent flow. Fig.(1) show the graphical form of jet –ejector that will be studied in this research and the specifications of this jet – ejector are shown in table 1.

The total kinetic energy before mixing is the sum of the kinetic energy between the motive and propelled stream. The kinetic energy of motive stream is [4]:

$$E = \frac{1}{2} m v^2 \quad \text{..... (1)}$$

and the continuity equations can be written as :

$$m = m_1 + m_3 \quad \text{..... (2)}$$

The velocity of the mixture stream is computed by momentum conservation. Because of finite computational resources and the flow behavior in jet ejectors, the standard *k-ε* model is the best compared to other schemes, so the standard *k-ε* model is applied throughout the study.

Assuming that the gas is compressible and viscous fluid, the conservation equations of its mass, momentum and energy can be written as[5]:

$$\frac{\partial}{\partial t}(\rho\varphi)+\frac{\partial}{\partial x}\left(\rho v_x\varphi-\Gamma_\varphi\frac{\partial\varphi}{\partial x}\right)+\frac{\partial}{\partial y}\left(\rho v_y\varphi-\Gamma_\varphi\frac{\partial\varphi}{\partial y}\right)+\frac{\partial}{\partial z}\left(\rho v_z\varphi-\Gamma_\varphi\frac{\partial\varphi}{\partial z}\right)=S_\varphi \quad \ldots(3)$$

where: ϕ =dependent variable (velocity components , temperature , both kinetic and dissipation energies). Γ_ϕ =effective exchange variable coefficient of ϕ . S_ϕ = source term with the total pressure gradient. Eddy viscosity must be determined on the basis of an adequate turbulent model . The standard *k-ε* model is a semi-empirical model for turbulent kinetic energy, k, and its dissipation rate, ε . The model assumes that the effects of molecular viscosity are negligible and the flow is fully turbulent.

The turbulence kinetic energy, *k*, and its dissipation rate, ε , are calculated from:

$$\frac{Dk}{Dt}=\frac{\partial}{\partial X_i}\left\{\left\{(\nu\delta_{jk}+c_s\frac{k}{\varepsilon}\bar{u}_k\bar{u}_j)\frac{\partial k}{\partial X_k}\right\}-\bar{u}_k\bar{u}_j\frac{\partial u_i}{\partial X_k}-\varepsilon \quad \ldots(4)$$

$$\frac{D\varepsilon}{Dt}=\frac{\partial}{\partial X_i}\left\{\left\{(\nu\delta_{jk}+c_1\frac{k}{\varepsilon}\bar{u}_k\bar{u}_j)\frac{\partial\varepsilon}{\partial X_k}\right\}-\frac{\varepsilon}{k}c_2\bar{u}_k\bar{u}_j\frac{\partial u_i}{\partial X_k}-c_3\varepsilon \quad \ldots(5)$$

Model constants: c_s , c_1 , c_2 , c_3 are 0.22 , 0.18 ,1.44 and 1.92 respectively[6].

The head ratio R_H is defined as the ratio of the operating head to the discharge head [7]:

$$R_H=\frac{(P_1-P_3)}{(P_5-P_3)} \quad \ldots(6)$$

The mass ratio can be expressed as[7]:

$$M=\frac{m_3}{m_1} \quad \ldots(7)$$

In completing a CFD analysis of the entire domain of the geometry, it is necessary to set up the governing equations. The governing equations could be solved with the aid of the following assumptions:

1. The flow is steady state.
2. The working fluid is air.
3. The flow is turbulent and compressible.
4. The ejector is at horizontal plane.
5. The properties of flow are constant.
6. The body forces are neglected.
7. Effect of heat transfer is neglected.
8. fully developed region at the inlet part.

Boundary conditions:

1- Nozzle inlet

Flow at the nozzle inlet upstream of the step is considered to be isothermal, hydrodynamically steady and fully developed with a distribution for the stream wise inlet pressure at values 1, 1.5, 2, 2.5, 3, 3.5, 4, 4.5, 5 and 5.5 bar

Wall: no slip velocity, constant temperature

$$\left.\begin{aligned}k_{in}&=C_k w_{in}{}^2\\ \varepsilon_{in}&=C_\mu k_{in}{}^{3/2}/(0.5D_hC_\varepsilon)\end{aligned}\right\}$$

Where C_k & C_ε are constants (C_k=0.003 & C_ε=0.03)[8] .

D_h: Hydraulic diameter

2- Outlet: The outlet pressure is zero**.** and out flow condition and fully developed conditions at the diffuser exit.

$$\frac{\partial u}{\partial x}=\frac{\partial v}{\partial x}=\frac{\partial k}{\partial x}=\frac{\partial\varepsilon}{\partial x}=0$$

4-Results & Discussion

This section includes details of computational results for the two dimensional,

hydrodynamics characteristics of turbulent flow in the ejector.

Fig. (2) illustrates the effect of the initial pressure upon ejector performance as a head ratio and mass ratio. The initial pressure is varied from 1 to 5.5 bar with 0.5 bar increment. Ejector mass ratio is less sensitive at the low region initial pressure while it decreasing with increasing the diameter ratio. As the initial pressure increases, the head ratio of the ejector is high effected also increases at low initial pressure up to 2.5 bar with diameter ratio, while at high initial pressure the head ratio decreases with increasing the diameter ratio reached to minimum value at 0.8 diameter ratio and it increased at higher diameter ratio.

Also the high effect of the initial pressure on the mass ratio at the low diameter ratio (small nozzle diameter) is indicated, while at high nozzle diameter no effect on the mass ratio due to the low throat after diameter ratio 0.8 . At low initial pressure a little effect of diameter ration on the heat ratio, while at high initial pressure there is high effect on it.

The effect of the initial pressure on the mass ratio with different diameter ratio is plotted in Fig.(3). The results show only high effect of initial pressure on the mass ratio at very low diameter ratio (0.125,0.25) while there is a little effect at the high diameter ratio due to excess into pressure drop at plane (4). Results indicate high mass ratio (M) at low diameter ratio (cases 1&2) with low static pressure.

Fig.(4) presents the effect of the initial pressure on the pressure ratio with different diameter ratio. At low initial pressure, all the diameter ratio are effected on the head pressure. There is significant effect of high diameter ratio (0.75) on the pressure ratio at high initial pressure.

Fig.(5) shows contour of the fluid velocity vector at the suction chamber with constant initial pressure 1bar and different diameter ratio. These results show the velocity distribution format in more than important section along the ejector. There is a significant effect in the section near the jet , so maximum velocity of the jet flow reached(480)m/s.

To increase understanding of the axial velocity distribution in an important regions along the ejector, the three regions are chosen at major proportion of structure. First plane at the inlet (line-in) region (1&3), second plane at the nozzle exit, region(2) while the third plane at the midpoint of the throat (line -2) region (4).

Fig.(6) shows the plot of velocity magnitude distribution along these three different planes at low diameter ratio 1/8 (case 1). At the midpoint of throat plane, region(4) (line -2) results show that the uniform profile of the velocity and maximum flow velocity reached to 500 m/s due to high diameter ratio which increased axial velocity at the nozzle exit and turbulent velocity profile has been created and the two streams combined into this section to create high velocity value, reached 500m/s.

. Low velocity appears at the nozzle inlet(1) compare to the suction inlet (3). The results show the existence of a significant increase in velocity at the center of the nozzle exit (2) due to the diameter ratio .

At the inlet regain(1&3) (line in), results indicate two different velocity values. At the inlet part parabolic distribution appear as a fully developed region while at the suction part the centrifuge interpose to great high velocity value near the inner wall (max velocity reach 400 m/s) (line-in). Also at the nozzle plane (2) results indicate two different velocity values. Maximum value appear at the nozzle neck, while reduces at the suction diameter.

Fig (7) presents the plot of velocity magnitude a cross three planes and constant diameter ratio is (0.25) case 2. At the inlet regain(1&3) (line-in), results indicate two different velocity values. The first part parabolic distribution appear as a fully developed region while at the suction part (3) the centrifuge interpose to great high velocity value near the inner wall as presented in Fig.6 (max velocity reach 500 m/s).Also at the nozzle plane results indicate two different velocity values. Maximum value appear at the nozzle neck, while reduces at the suction diameter. Finally at the least part (line-2) the

two streams combined into this section to great high velocity value reached 680m/s.

Figs.(8),(9) and(10) show the velocity magnitude value at cases (DN/DT)3/8, 5/8 and 7/8 respectively. Results show the axial flow through the nozzle increased with increasing the diameter ratio at all planes and high effect of turbulence flow at these cases. Maximum flow though nozzle plane reached 1200 m/s. At case(5) DN/DT 5/8 indicates the high jet performance due to increase into the suction flow (3), while the parabolic profile is appeared at the plane (1) due to increase into the flow velocity.

Fig.(11) presents velocity magnitude distribution at case (8) DN/DT=8/8. At the nozzle diameter increased, the velocity profile is formed as parabolic from case 5 reached to uniform profile at case 8. Results present turbulent velocity profile at uniform tube into the fully developed region, due to the different reasons.1-turbulent velocity distribution curve appears at nozzle plane . 2-Both nozzle and outlet plane (line -2) reached equal maximum velocity.3- The inlet plane at nozzle part presents the maximum value than other cases.

5-Conclusions:

The most important conclusions that can be drawn from the present study are as the following:

1- At increase the nozzle diameter ratio suction flow also increased until to diameter ratio reach 8/8 as shown in Fig.(11) .
2- The head ratio at low initial pressure (less than 2 bar) have inverse behavior when the inlet pressure will be high (great than 3 bar)
3- The jet – ejector selected in this research have cutting in mass ratio at nozzle to throat diameter ratio reaches to 0.8 as shown in Fig.(2)
4- The greater mass ratio occurs when the nozzle to throat diameter ratio was 0.125,case (1) due to high jet velocity at nozzle exit and the increased the suction at the motive fluid (m3).
5- The higher pressure ratio occurs when the nozzle to throat diameter ratio was 0.625,case (5).

6-References

[1] Shengqiang Shen , Xiaoping Qu, Bo Zhang, Saffa Riffat and Mark Gillott "Study of a gas–liquid ejector and its application to a solar-powered bi-ejector refrigeration system" Applied Thermal Engineering 25 (2005) 2891–2902

[2] Huang, . Chang, Wang and Petrenko "A 1-D analysis of ejector performance" International Journal of Refrigeration 22 (1999) 354–364

[3] Mark J. BERGANDER " refrigeration cycle with two-phase condensing ejector" International Refrigeration and Air Conditioning Conference at Purdue, July 17-20, 2006

[4] Zhang, X.J. and Wang, R.Z " A new combined adsorption–ejector refrigeration and heating hybrid system powered by solar energy" Applied Thermal Engineering 22 (2002) 1245–1258.

[5] Kanjanapon Chunnanond and Satha Aphornratana " Ejectors: applications in refrigeration technology" Renewable and Sustainable Energy Reviews 8 (2004) 129–155

[6] Hisham El-Dessouky , Hisham Ettouney, Imad Alatiqi and Ghada Al-Nuwaibit "Evaluation of steam jet ejectors" Chemical Engineering and Processing 41 (2002) 551–561

[7] Igor J. Karassik, Joseph P. Messina, Paul Cooper and Charles C. Heald "pump handbook" third edition,

[8] Ayad Mahmoud Salman, “Turbulent Forced Convection Heat Transfer in the Developing Flow through Concentric Annuli”, Mechanical Engineering Department of University of Technology, July 2003.

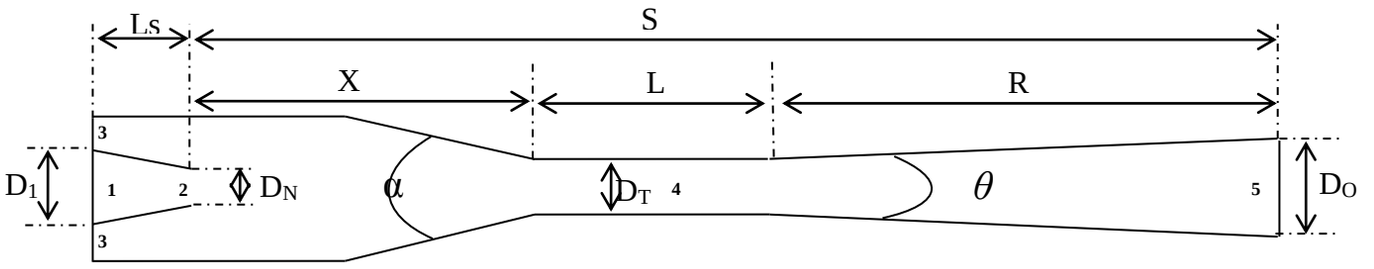

Figure.1 The ejector geometry with the important dimensions.

Table 1 the options of jet – ejector are using in this research

Symbol	D_T	S	D_1	R	X	L	Ls	D_N/D_T	θ	α
Value	*6.98 mm*	$15D_T$	D_T	$12D_T$	$2D_T$	$4.5D_T$	$2.25D_T$	From 1/8 to 8/8	5^o	28^o

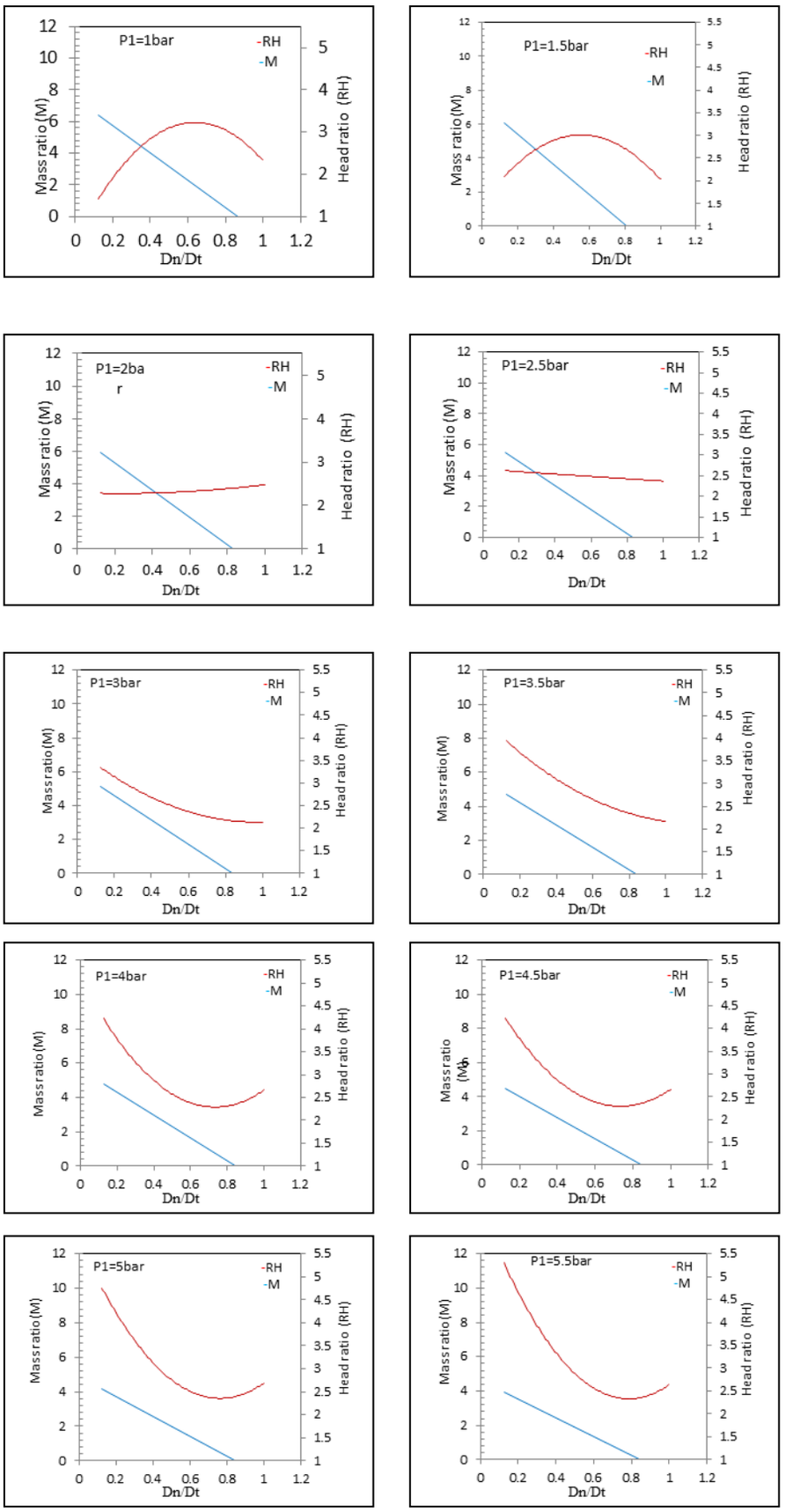

Figure. 2 The ejector performance with different initial pressure and diameter ratio

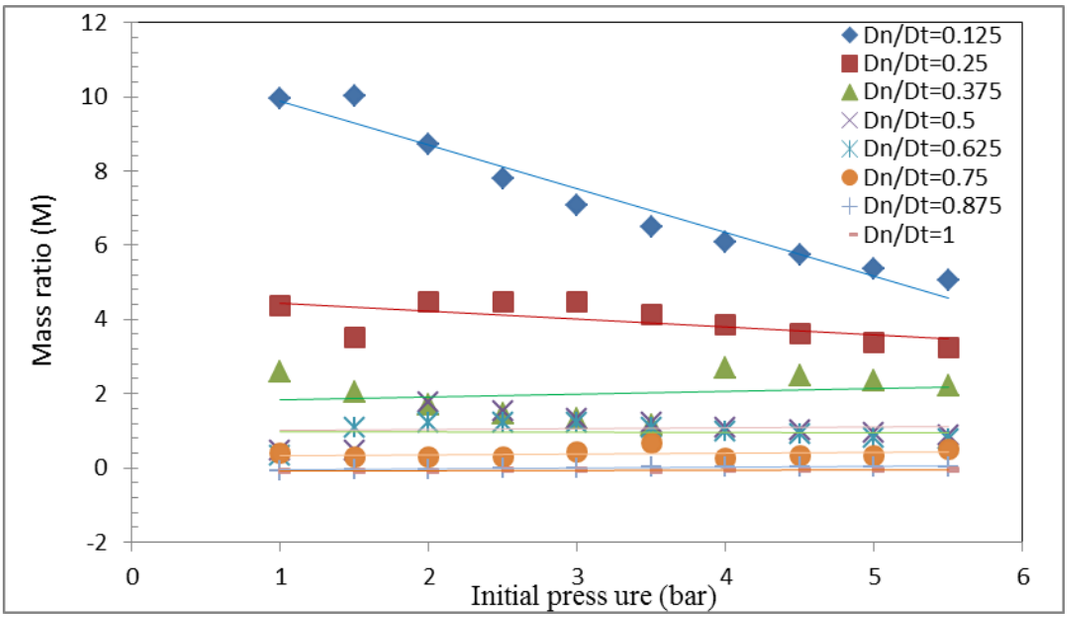

Figure. 3 The effect of the initial pressure on the mass ratio with different diameter ratio

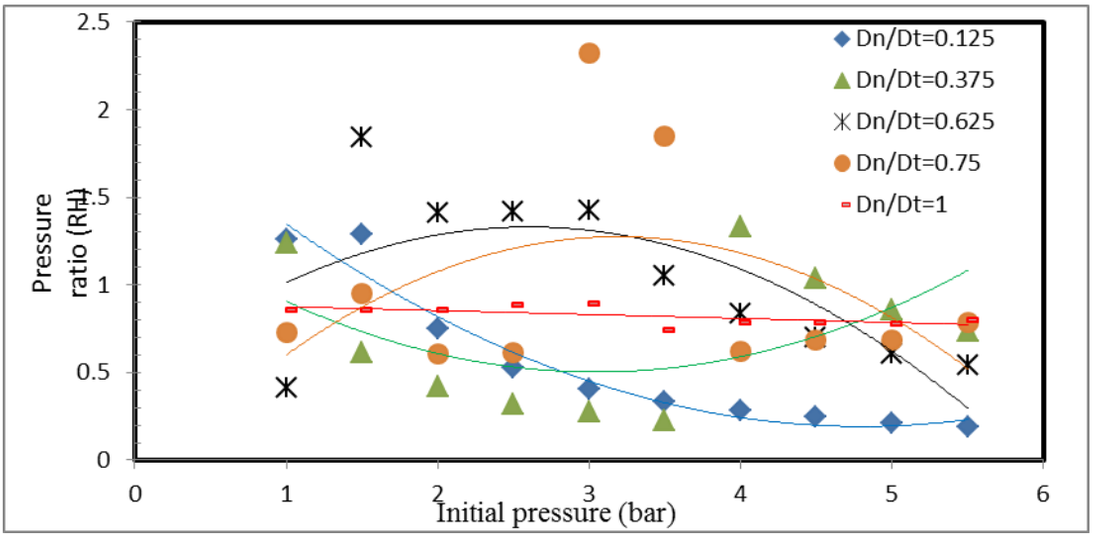

Figure. 4 The effect of the initial pressure on the mass ratio with different diameter ratio

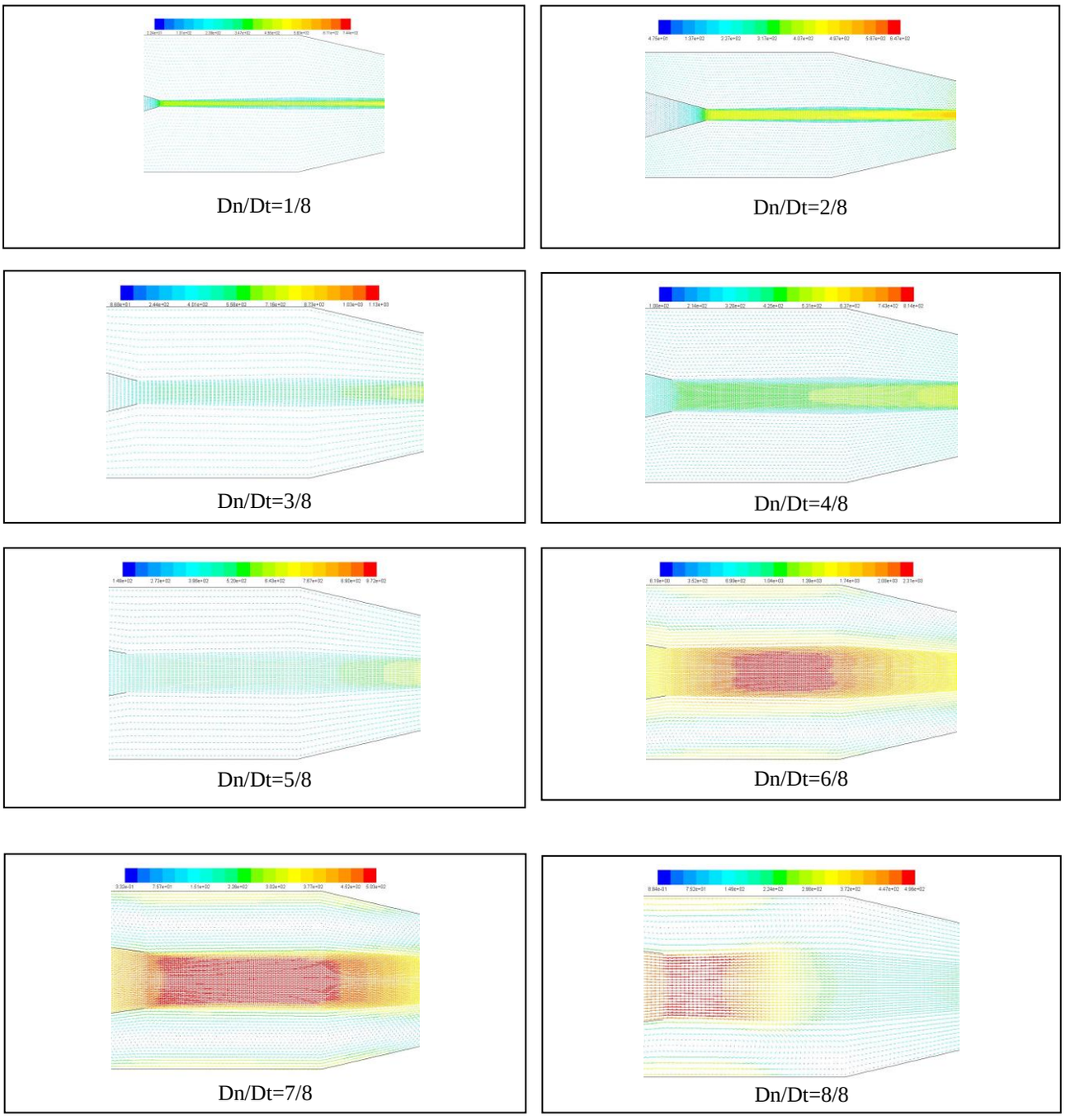

Figure .5 Fluid velocity vector contour at the suction chamber at constant initial pressure 1bar with different diameter ratio(eight cases)

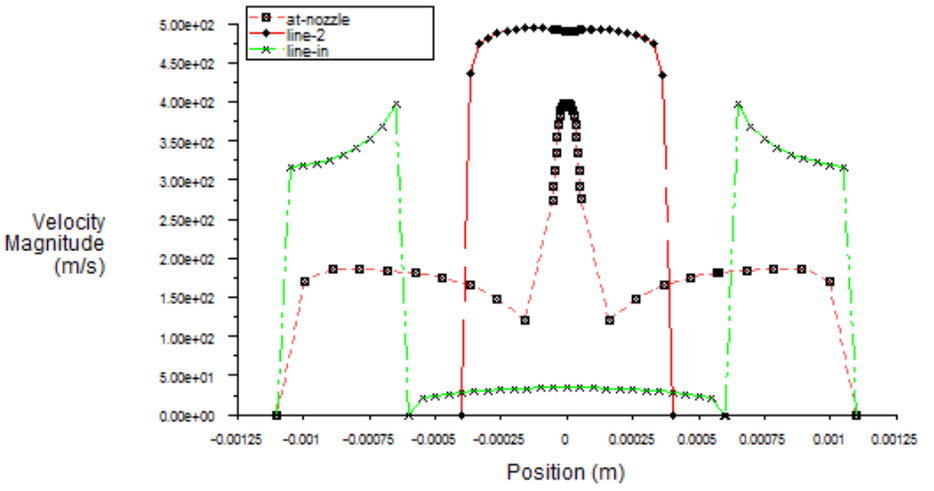

Figure.6 Velocity magnitude distribution along three different positions along the ejector diameter: case 1(D_N/D_T=1/8).

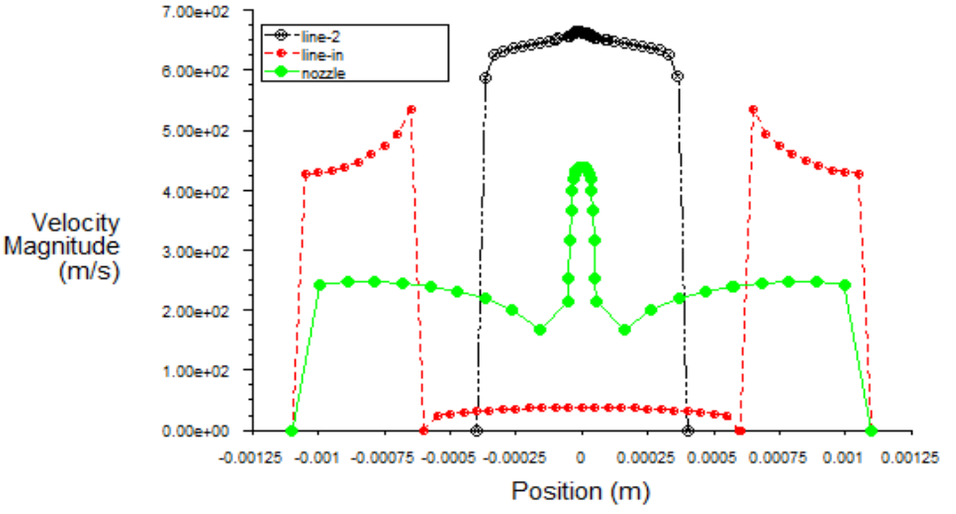

Figure.7 Velocity magnitude distribution along three different positions along the ejector diameter: case 2 (D_N/D_T=2/8).

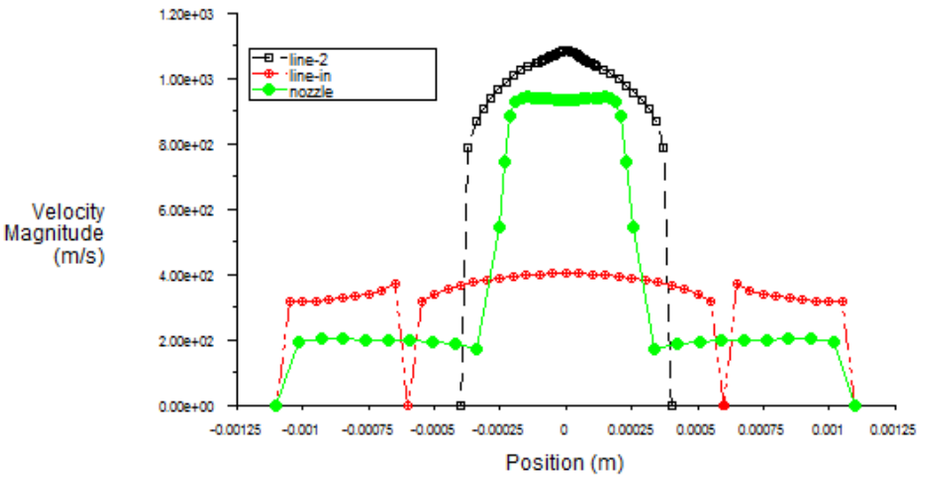

Figure.8 Velocity magnitude distribution along three different positions along the ejector diameter: case 3 (D_N/D_T=3/8).

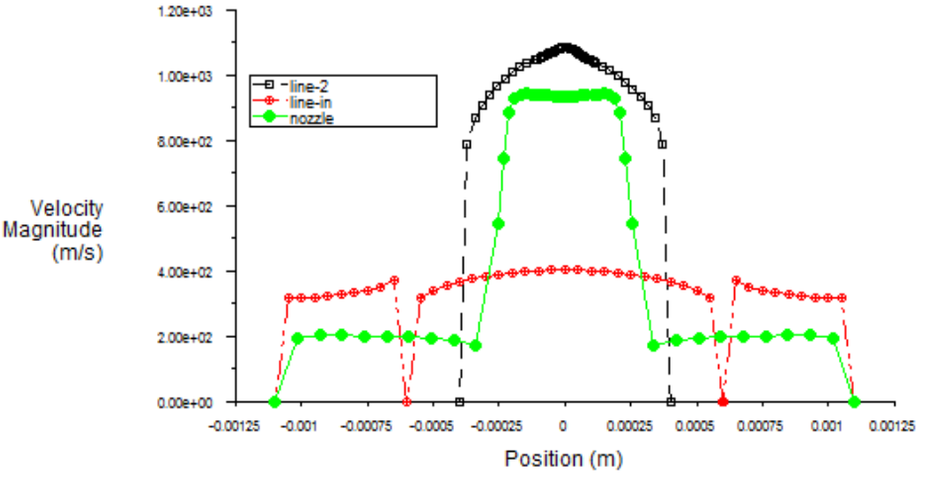

Figure.9 Velocity magnitude distribution along three different positions along the ejector diameter: case 5(D_N/D_T=5/8).

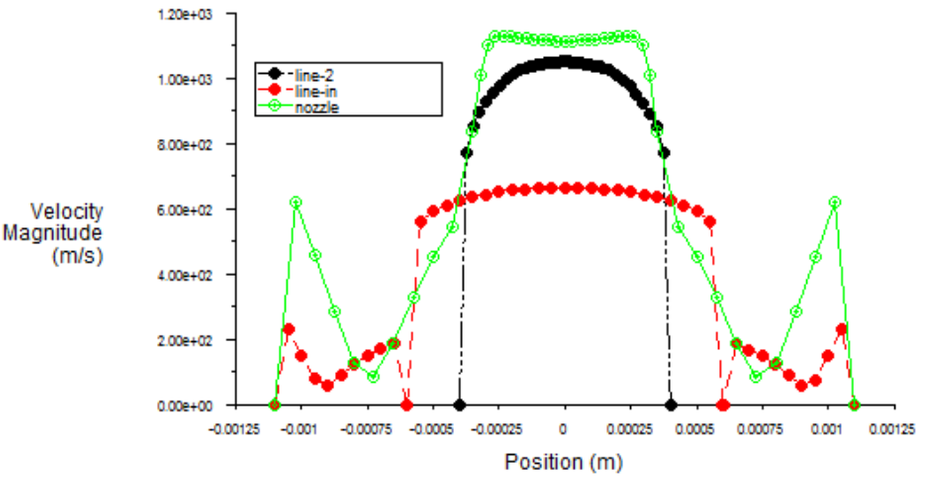

Figure.10 Velocity magnitude distribution along three different positions along the ejector diameter: case 7 (D_N/D_T=7/8).

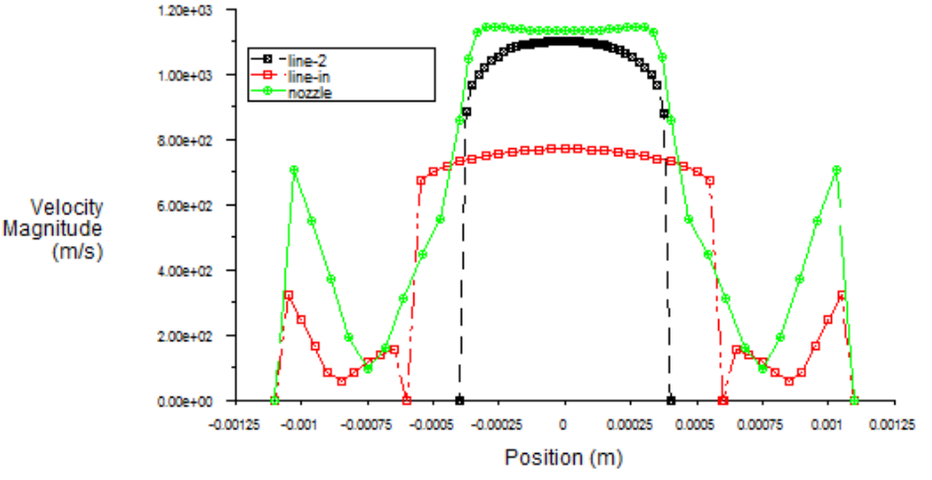

Figure.11 Velocity magnitude distribution along three different positions along the ejector diameter:case8 (D_N/D_T=8/8).